Food Hydrocolloids 137 (2023) 108401

Contents lists available at ScienceDirect

Food Hydrocolloids

journal homepage: www.elsevier.com/locate/foodhyd

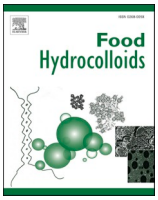

Fluid gels' dual behaviour as granular matter and colloidal glass

Gabriele D'Oria [a], Deniz Z. Gunes [b,**], François Lequeux [c], Christoph Hartmann [d], Hans Joerg Limbach [d], Lilia Ahrné [a,*]

[a] Department of Food Science, Faculty of Science, University of Copenhagen, Rolighedsvej 26, DK-1958, Frederiksberg C, Denmark
[b] Department of Chemical Engineering and Center for Food and Microbial Technology, KU Leuven, 3001, Leuven, Belgium
[c] Laboratoire Sciences et Ingénierie de la Matière Molle, CNRS UMR7615, ESPCI Paris, PSL Research University, 10 rue Vauquelin, F-75231, Paris, France
[d] Nestlé Research, Vers-Chez-Les-Blanc, 1000 Lausanne 26, Switzerland

ARTICLE INFO

Keywords:
Rheology
Time dependency
Yield stress
Ageing
Ripening

ABSTRACT

Fluid gels are jammed suspensions made of deformable particles obtained by applying shear during the sol-gel transition of a hydrocolloid. Their rheological properties have been shown to be subject to large uncertainty and to change over time undergoing an ageing process. In the present fluid gel literature, it is not known whether such ageing is due to physical ageing, formation of new ion bridges, gravitational effects, or a type of ripening. Methodologies were developed to understand and quantify the fluctuations in the rheological properties of the systems investigated, which were shown to be intrinsic to their jammed particulated microstructure and reminiscent of granular matter. In addition, the time dependent evolution of the rheological properties of fluid gels have been investigated in detail. For the first time, our work determined that the time evolution of the relaxation time is not due to the ripening of the particles, to new ion bridges, and not caused by gravity-induced effects. Our results instead suggest that is caused by physical ageing which is a behaviour reminiscent of colloidal glasses. In this regard, the present study aims not only to support future systematic rheological analysis, considering the intrinsic fluctuations and the time dependency of the rheological properties, but also serves as an aid to successfully design and scale-up industrial applications.

1. Introduction

Fluid gels are produced by applying shear to a gelling hydrocolloid solution during the sol-gel transition. As a result, microgel particulate suspensions above the random close packing point are obtained (Brown, Cutler, & Norton, 1996). The academic and industrial relevance of fluid gels derives from their remarkable material properties, e.g. the presence of yield stress (σ_y) (García, Alfaro, & Muñoz, 2015; Garrec, Guthrie, & Norton, 2013; Sworn, Sanderson, & Gibson, 1995), a pronounced shear thinning behaviour (Bagheri, Mousavi, & Madadlou, 2014; García, Trujillo, Muñoz, & Alfaro, 2018; Garrec et al., 2013; Sworn et al., 1995) and a major elastic response within the linear viscoelastic region (García et al., 2018; Ghebremedhin, Seiffert, & Vilgis, 2021). In addition, fluid gel particles are surrounded by a non-gelled low viscous continuous phase (Cassin, Appelqvist, Normand, & Norton, 2000; Fernández Farrés, Moakes, & Norton, 2014). Those properties can be tuned by process and formulation parameters (Gabriele, Spyropoulos, & Norton, 2009; Ghebremedhin et al., 2021; Norton, Jarvis, & Foster, 1999), and made fluid gels attractive as a suspending agent (Bagheri et al., 2014; Qin, Ma, Li, & Li, 2017), viscosifier (Bagheri et al., 2014; Fernández Farrés, Douaire, & Norton, 2013; Garrec et al., 2013), foam stabiliser (Ellis, Mills, Norton, & Norton-Welch, 2019), satiety modulator (Bradbeer, Hancocks, Spyropoulos, & Norton, 2015; Norton, Frith, & Ablett, 2006) and tactile-sensation improver (Fernández Farrés et al., 2013; Fernández Farrés & Norton, 2015; Garrec & Norton, 2013; Mahdi, Conway, Mills, & Smith, 2016) in many different application fields.

Once fluid gels have been produced, their elastic modulus G' has been shown to increase with time (Caggioni, Spicer, Blair, Lindberg, & Weitz, 2007; Fernández Farrés & Norton, 2014; Gabriele et al., 2009; García et al., 2015; Sworn et al., 1995). Being fluid gels jammed suspension made of gelled particles, such increase can possibly be caused by a fluid gel intra-particle microstructural evolution or by fluid gel inter-particle interactions. In the context of this manuscript, we refer to *ripening* as the fluid gel intra-particle structural evolution of the gel

* Corresponding author.
** Corresponding author.
E-mail addresses: deniz.gunes@kuleuven.be (D.Z. Gunes), lilia@food.ku.dk (L. Ahrné).

https://doi.org/10.1016/j.foodhyd.2022.108401
Received 18 September 2022; Received in revised form 23 November 2022; Accepted 7 December 2022
Available online 20 December 2022

network, and to *physical ageing* as the process occurring at the inter-particle microstructural level.

So far in the literature, the increase of G′ with time has been speculatively associated with 1) fluid gel inter-particle post-processing ordering process caused by the polymer coils sitting at the particle surface, if the gelation process was entirely performed under shear and associated with 2) fluid gel particle-particle aggregation and subsequent quiescent gel network formation, if the shear stopped before the completion of the fluid gel particle formation (Fernández Farrés et al., 2014). In studies of concentrated suspensions, not specific to fluid gels, G'(time) increase has been pointed out as a colloidal glass signature (Emady, Caggioni, & Spicer, 2013; Joshi & Petekidis, 2018), i.e. these systems are unable to reach a thermodynamic equilibrium at the level of the particle motion within the suspension. Colloidal glassy systems are characterised by slow dynamics which passes between metastable states of lower and lower energies. This phenomenon, known as physical ageing, causes the physical properties of glassy systems to slowly evolve with waiting time t_w i.e. physical ageing causes an increase of the relaxation time with waiting time, which has been modelled by a power law function in former literature (Cloitre, Borrega, & Leibler, 2000; Struik, 1977; Hodge, 1995; Joshi & Petekidis, 2018). The application of a deformation field, usually aimed at inducing partial or full rejuvenation, has been shown to respectively decelerate or even remove the effects caused by physical ageing (Viasnoff & Lequeux, 2002), i.e. the evolution of the rheological properties induced by physical ageing is potentially erased by rejuvenation.

Previous research on quiescently gelled hydrocolloids reported that after gel formation, complete ripening of the gel network usually takes hours, or even days, until a stable gel structure is completely created. The increase in elastic modulus G'(time) in biopolymeric gel systems has been associated with continuous formation and rearrangement of the junction zones due to hydrogen bonds and hydrophobic interactions in high methoxyl pectin/sucrose systems (Lopes da Silva & Gonçalves, 1994) and with further development of already formed cross-links in bovine gelatine (Normand, Muller, Ravey, & Parker, 2000). It is usually assumed that such process might occur similarly within the gel structure of individual fluid gel particles. Thus, in previous studies on fluid gels, a common practise has been to store the samples for a certain time – typically between 24 and 48 h – before any rheological test was performed to allow such process to happen (Di Napoli et al., 2020; Gabriele et al., 2009; García et al., 2015, 2018; Garrec et al., 2013; Garrec & Norton, 2012; Ghebremedhin et al., 2021).

Fluid gels' properties have been usually assessed by measuring their rheological characteristics. Amplitude sweeps and frequency sweeps have been used to determine the linear viscoelastic region and mechanical spectrum (Fernández Farrés et al., 2013; Garrec & Norton, 2012; Ghebremedhin et al., 2021), respectively whereas, stress ramps (Fernández Farrés et al., 2013; Gabriele et al., 2009) and creep measurements (Fernández Farrés et al., 2013; García et al., 2015; Garrec & Norton, 2012) were used to determine the yield stress σ_y. When measuring the latter property, large standard deviations have been reported for both gellan gum fluid gels (García et al., 2015) and κ-carrageenan fluid gels (Garrec & Norton, 2012). Such lack of repeatability has been suggested to be due to a marked shear thinning region and to the onset of shear banding (i.e. flow-induced structuring where parallel bands of different structures and viscosities are coexisting in the sample) due to the heterogeneous microstructure of fluid gels (García et al., 2015). Such heterogeneity could possibly derive from their granular matter nature at the particle level, as first described by Cassin et al. (2000). Granular materials are non-colloidal systems where thermodynamic aspects can be neglected due to the size of the particles forming the system. These matrixes are subject to intrinsic fluctuations in their packing density when their packing is observed following the application of flow (Nowak, Knight, Ben-Naim, Jaeger, & Nagel, 1998). They can compact if exposed to intermittent external stresses (Kabla & Debrégeas, 2004) and display the characteristic sandpile-like conical structures, namely granular piles (Vanel, Howell, Winters, Behringer, Clément, 1999).

From the former fluid gel literature, it becomes apparent that such systems are complex and multi-scale matrixes e.g. colloidal at the polymer coil level and granular at the particle level and therefore, an approach is required to take this duality into account. In this study, we aim to draw a more precise description of fluid gels as a granular material investigating the origin of fluctuation in the rheological properties, the presence of granular pile formations and intermittent packing. In this regard, the uncertainty of rheological properties was investigated and quantified, developing a cycle-based protocol that takes fluctuations into account to provide more reproducible results. In addition, we aim at studying more clearly whether the G′(time) increase is due to physical ageing, formation of new divalent ion bridges by studying both fluid gels formed via ionic and non-ionic gelation, ripening or gravity-induced effects by manipulating the density of fluid gel particles entrapping silica inclusions. It is hypothesised that the developed method will allow a quantification of the effect of ageing on fluid gel's rheology and dynamics, allowing to build a model to predict the evolution of the system in the absence of perturbation. Furthermore, we aim at providing a multi-scale approach in the methods proposed to obtain more reproducible results and foster fluid gel industrialisation by determining fluctuations in rheological properties and by describing, controlling, and predicting the ageing effects.

2. Materials and methods

2.1. Fluid gel production

2.1.1. Low acyl (LA) gellan gum fluid gels

The LA gellan gum fluid gels investigated were produced by first mixing 0.0999 ± 0.0001% w/w LA gellan gum (Kelcogel® F™) provided by CP Kelco (San Diego, USA) to 70 °C Milli-Q water (conductivity at 25 °C = 0.056 μS/cm). The sample was left to stir at 70 °C for 25 min in a glass beaker covered by aluminium foil to prevent water evaporation. The hydration temperature chosen ensured a correct hydration of gellan gum given the gellan concentration and medium used (Valli & Miskiel, 2001). Then, a 0.1 M calcium chloride solution was added to reach a final concentration of 5.5 mM. The sample was left to stir until its temperature reached again 70 °C. Subsequently, it was transferred to the rheometer DHR – 2 (TA Instruments, New Castle, USA) to be processed with a vane and sanded cup setup, which was previously heated to 70 °C. The cup was covered by a lid to limit water evaporation. Thereto, the solution was left to equilibrate at 70 °C for 5 min, followed by stirring at 500 s^{-1} while cooling down from 70 to 20 °C at a cooling rate of 0.5 °C/min.

2.1.2. LA gellan gum fluid gels with silica microparticles inclusions

Silica microparticles of 750 nm (Fiber Optic Center, New Bedford, USA) were dispersed in Milli-Q water at different concentrations (0.04, 0.15, 0.5, 2, 7, 10% w/w). To aid the dispersion of silica in Milli-Q water the silica and water mixture was processed with the help of an ultrasonic processor (UP400St, Hielscher, Teltow, Germany) with six cycles of 10 min at 130W. To avoid excessive evaporation, the samples were left at rest 5 min in between ultrasonication cycles and covered with aluminium foil during the whole ultrasonication process. In the case of 10% w/w silica, 9 ultrasonication cycles were performed to allow a better dispersion of the silica particles. The silica dispersions were then heated to 70 °C and 0.0999 ± 0.0001% w/w LA gellan gum was added to the sample and left to stir at 70 °C for 25 min. Thereto, a 0.1 M calcium chloride solution was added to the sample until a final concentration of 5.5 mM was reached. The temperature was left to equilibrate to 70 °C. Hence, the sample was processed in the rheometer using the vane and sandblasted cup. The setup was covered with a lid to limit water evaporation and the sample was left to equilibrate to 70 °C for 5 min. Hence, it was processed at 500 s^{-1} while cooling down from 70 to

20 °C at a cooling rate of 0.5 °C/min.

2.1.3. Agar fluid gels

Agar powder (Sigma-Aldrich, St. Louis, USA) was added to reach a concentration of 0.4% w/w to Milli-Q water at room temperature while it was mixed by a magnetic stirrer. The sample was then heated to 90 °C to ensure complete hydration of the hydrocolloid, covering the beaker with aluminium foil to prevent excessive evaporation. The liquid was transferred to a preheated rheometer sandblasted cup, where it was cooled down from 90 to 20 °C at a cooling rate of 0.5 °C/min while shearing at 500 s^{-1}. Then, the sample was kept at the same shear rate for 15 min at 20 °C.

2.1.4. Fluid gel storage after production

Once produced, the fluid gel samples were poured in falcon tubes and stored for 48 h in a cooled incubator (INCU-Line® 68R, VWR International, Radnor, USA) at 20 °C (±0.1) before any further test was performed.

2.2. LA gellan gum quiescent gel production and ripening

The LA gellan gum quiescent gel was manufactured by first heating up Milli-Q water to 70 °C in a glass beaker covered by aluminium foil. Thereto, 0.0999 ± 0.0001% w/w LA gellan gum was added to the water and left to stir for 25 min. Calcium chloride was added to the sample from a 0.1 M stock solution until reaching a final concentration of 5.5 mM. The temperature was allowed to raise back to 70 °C. Hence, the sample was transferred to a rheometer sandblasted concentric cylinder setup, which was preheated to 70 °C. The liquid was covered with a layer of paraffin oil and a lid to avoid excessive evaporation during testing. The temperature was equilibrated at 70 °C for 5 min. After this step, a strain of 0.1% was applied at a frequency of 1 Hz while the sample was cooled down from 70 to 20 °C at a cooling rate of 0.5 °C/min. Once the temperature reached 20 °C, it was not decreased further and a strain of 0.1% at 1 Hz was performed to investigate the ripening of the LA gellan gum quiescent gel produced for over 59 h.

2.3. Rheological characterisation

The stress-controlled DHR – 2 rheometer (TA Instruments, New Castle, USA) was used for the rheological characterisation performed in this study. The tests were executed at 20 °C using a sanded concentric cylinder geometry to prevent wall slip. After loading the sample, a rejuvenation step was applied at 1000%, 1 Hz for 10 s to delete the loading history and system's ageing. The choice of using a large amplitude rejuvenation in oscillation mode is due to the fact that we want to revive the system without affecting its shear memory. Indeed, performing the rejuvenation in oscillation mode with an even number of cycles allows to minimise the relaxing strain from such step. In that respect, our protocol differed from the one used by Cloitre et al. (2000) and Lidon, Villa, and Manneville (2017).

In the present study, time is intended as the period from the start of the rheological test, waiting time (t_w) is defined as the time elapsed from the last rejuvenation step and finally, resting time describes the time passed from the end of fluid gel production.

2.3.1. Amplitude sweep

After a rejuvenation step, an amplitude sweep from 0.01% to 1000% at 1 Hz was performed to probe the elastic modulus G' within the LVR and the yield point of the system. The latter was determined by the tangent intersection method (Völp et al., 2021; Willenbacher & Lexis, 2018). An example is showed in Fig. S1 (supplementary material) where the tangent crossing point indicates the yield stress σ_y of the sample tested.

2.3.2. Investigation of LA gellan gum fluid gel ripening

LA gellan gum fluid gels were manufactured following the protocol described in section 2.1. Thereto, the samples were stored in a cooled incubator at 20 °C before testing for three different resting times: 1, 4 and 48 h. The elastic modulus of the fluid gels at different resting times was analysed using the amplitude sweep method described in section 2.3.1.

2.3.3. Investigation of fluid gel ageing dynamics

Fluid gel ageing dynamics were assessed with two methods. *Time sweep*: after a rejuvenation step, a strain within the linear viscoelastic region (0.3% for LA gellan gum fluid gels and 0.1% for agar fluid gels) was imposed at a frequency of 1 Hz for 10000 s to study the evolution of G′ over time. *Repeated creep*: a cycle composed of the following three steps was designed: 1) a rejuvenation step to delete the sample's history, 2) a waiting time (t_w) step where no stress was applied for a certain time and 3) a creep step σ_{cr} in which a stress (0.05 Pa for LA gellan gum fluid gels and 0.1 Pa for agar fluid gels) below the yield stress σ_y was applied for 1000 s (Fig. 1). This 3-steps protocol was repeated in cycles to gain statistical resolution on the fluid gel ageing dynamics of LA gellan gum and agar fluid gels (Table 1) and of LA gellan gum fluid gels entrapping silica microparticle inclusions (Table 2). Paraffin oil (VWR International, Radnor, USA) was added on top of the samples to prevent water evaporation during the measurements. Paraffin oil has been used on LA gellan gum fluid gels for waiting times of 3000 and 6000 s and for agar fluid gels for waiting times of 300, 1000, 3000 and 6000 s.

The relaxation time τ, from the creep in step 3, was retrieved using the stretched exponential model given by Equation (1). Two fit parameters were used in aforementioned model: τ, the relaxation time of the system and α, the stretch exponent. The stretch exponent α was chosen to be a fit parameter in order to retrieve the relaxation spectrum width of the experimental data. In addition, two parameters were imposed when modelling the experimental data: γ_0, the strain measured in step 3 after 10 s from its start (it was chosen to consider the data after 10 s from the creep start to eliminate the creep ringing region (Ewoldt & McKinley, 2007)), γ_∞, the strain measured at the end of step 3.

$$\gamma = (\gamma_0 - \gamma_\infty)[exp\ (-t/\tau)^{\alpha}] + \gamma_\infty \quad 0 < \alpha \leq 1 \tag{1}$$

The data measured using the repeated creep protocol described above and summarised in Fig. 1 were analysed to retrieve the fluid gel ageing dynamics by looking at: 1) the relaxation time τ as function of waiting time (t_w), 2) the stretch exponent α as function of t_w, 3) the delta $\gamma_\infty - \gamma_0$ versus t_w, 4) the instantaneous elastic response G evolution as function of the number of cycles performed at a specific t_w and 5) the

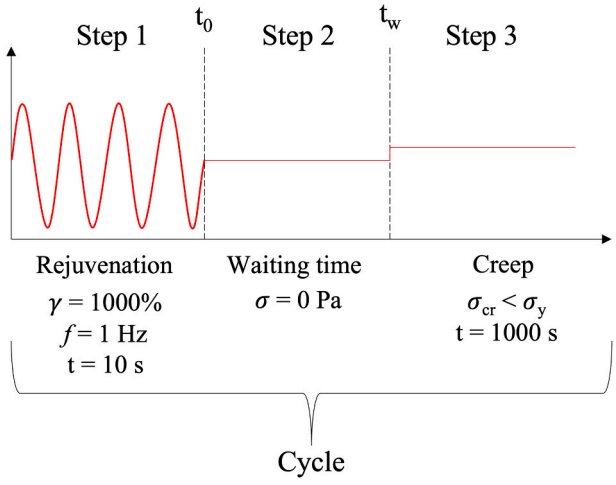

Fig. 1. Schematic representation of the repeated creep method, on which the determination of $\tau(t_w)$ and $\alpha(t_w)$ is based.

Table 1
Number of cycles repeated for each waiting time t_w for LA gellan gum and agar fluid gels.

t_w (s)		5	30	90	300	1000	3000	6000
Number of cycles	LA gellan gum fluid gel	77	93	61	58	77	100	49
	Agar fluid gel	–	73	–	74	72	60	17

Table 2
Number of cycles performed for LA gellan gum fluid gel samples manufactured with silica dispersions at different concentrations.

Silica dispersion concentration (% w/w)	0.04	0.15	0.5	2	7	10
Number of cycles ($t_w = 90$ s)	70	80	77	75	80	92

evolution of the relaxation time τ versus the number of cycles performed at a set t_w.

2.4. Gaussian fitting of $\tau(t_w)$ dataset

The $\tau(t_w)$ dataset obtained from the repeated creep method (described in section 2.2) was analysed to retrieve the data distribution. Firstly, the average and the standard deviation of the dataset was calculated. Then, the data were divided into bins. The number of bins into which the data distribution was categorised into was calculated with the aid of Sturges' rule $\lceil \log_2 o + 1 \rceil$, where o is the number of observations. Sturges' rule is a formula commonly used to provide guidance when building frequency distribution curves (Scott, 2009). The probability function of the $\tau(t_w)$ data was calculated. Thus, ten thousand numbers were generated using the function "random data generator" using Excel®. It was imposed that the generated numbers should follow a gaussian distribution with the same average and standard deviation of the dataset. Hence, the numbers were classified into bins and the resulting fit was then plotted. All the obtained probability function distributions were normalised by their amplitudes.

2.5. LA gellan gum fluid gel nominal concentrations investigated

LA gellan gum fluid gels manufactured using the protocol described in section 2.1.1 were centrifuged (Sorvall RC 6, Thermo Fisher Scientific, Waltham, USA) at 10000 g for 10 min at 20 °C to separate the supernatant and the sediment. Hence, the two phases were remixed until reaching the nominal concentration desired. In this study, we investigated four different nominal concentrations: 1x, 1.5x, 2x and 3x.

2.5.1. Investigation of concentrated LA gellan gum fluid gels

Concentrated LA gellan gum fluid gels were obtained following the protocol described in section 2.5. The relaxation time τ of the concentrated samples was probed by using the repeated creep method (section 2.3.3) setting the waiting time $t_w = 90$ s. To measure the creep behaviour in the 1.5x, 2x and 3x concentrated samples the stress applied was adjusted to 0.1, 0.2 and 0.7 Pa, respectively. The number of cycles performed for 1.5x, 2x and 3x was 63, 78 and 63, respectively.

2.6. Bulk densitometry

The density difference $\Delta\rho = \rho_d - \rho_c$ between the dispersed (ρ_d) and the continuous phase (ρ_c) was measured with a densitometer (DMA 4500 M, Anton Paar, Graz, Austria) at 20 °C. The density of the dispersed phase ρ_d was estimated by measuring the fluid gel bulk density. Hence, such measurement assumed that the fluid gel particle density is also constituted by some continuous phase present between the fluid gel particle arms located around the particle core. Before measuring the dispersed phase density ρ_d, the samples were stirred to ensure a more homogeneous dispersion. The fluid gel continuous phase density (ρ_c) was measured, after the supernatant (continuous phase) was separated by centrifugation at 10000 *g* for 10 min at 20 °C as described in section 2.5.

2.7. Fluid gel imaging

LA gellan gum fluid gels: the samples were diluted 20 times with Milli-Q water before addition of 200 μL of 0.1% w/w of a cationic dye, toluidine blue O (Sigma-Aldrich, St. Louis, USA), which was used to stain the microgel particles contained in the fluid gels. Then, the samples were observed with a brightfield macroscope (Leica M10, Leica Camera AG, Wetzlar, Germany).

Agar fluid gels: after a 50 times dilution with Milli-Q water, 400 μL of 0.1% w/w of toluidine blue O dye were added to the samples. The specimens were then observed using a brightfield microscope (Leica M10, Leica Camera AG, Wetzlar, Germany). Thus, the images were processed using the software Fiji (v. 2.3.0/1.53f) to add the scale bar and split the RGB channels.

2.8. Estimation of gravitational stress

The gravitational stress σ_g was calculated using Equation (2) for fluid gels manufactured at different silica concentrations:

$$\sigma_g = \varphi(\Delta\rho)gL \quad (2)$$

where φ is the effective volume fraction of hard monodispersed spheres considered to be at random close packing = 0.64, $\Delta\rho$ is the difference between the bulk fluid gel density and the density of the supernatant measured using the protocol described in section 2.6, g is the gravitational constant and L is the characteristic length of the rheometer geometry used.

3. Results and discussion

3.1. Granular aspects of fluid gel rheology and microstructure

The processing method and conditions used produced LA gellan gum fluid gels and agar fluid gels with very anisotropic particulate structures (Fig. 2), exhibiting "arms" of colloidal nature (diameter in the order of 1 μm). LA gellan gum particles (Fig. 2a and b) are around five times larger than the agar particles (Fig. 2c and d) and they have different shapes. LA gellan gum and agar fluid gel show a viscosity(temperature) profile during processing that could be divided into three distinguished regions (Fig. S2, supplementary material): Region 1 indicates the stage before the sol-gel transition has occurred, region 2 shows the main sol-gel transition phase followed by region 3 where the main sol-gel transition has occurred (Gabriele et al., 2009). LA gellan gum fluid gel presents a faster transition from region B to region C of the formation profile and a lower overall viscosity during processing compared to the agar fluid gel (Fig. S2, supplementary material).

The formation of very anisotropic structures (Fig. 2) resulted from a processing where the shear forces dominated over the thermodynamic contributions, inhibiting the structural relaxation to a more spherical shape. The remarkable size difference between LA gellan gum and agar particles could be explained by two differences in the formation profile: 1) a faster sol-gel kinetics and 2) a lower overall viscosity during processing. The rate of molecular ordering during the sol-gel transition has been formerly suggested to have a relevant impact on the morphology and size of the fluid gel particles. Indeed, a faster molecular ordering results in larger and more anisotropic structures (Garrec & Norton, 2012). Multiple studies have also indicated that higher viscosities during fluid gel production result in smaller particle size due to higher shear stresses exerted on the forming particles (Fernández Farrés et al., 2014; Garrec & Norton, 2012; Ghebremedhin et al., 2021).

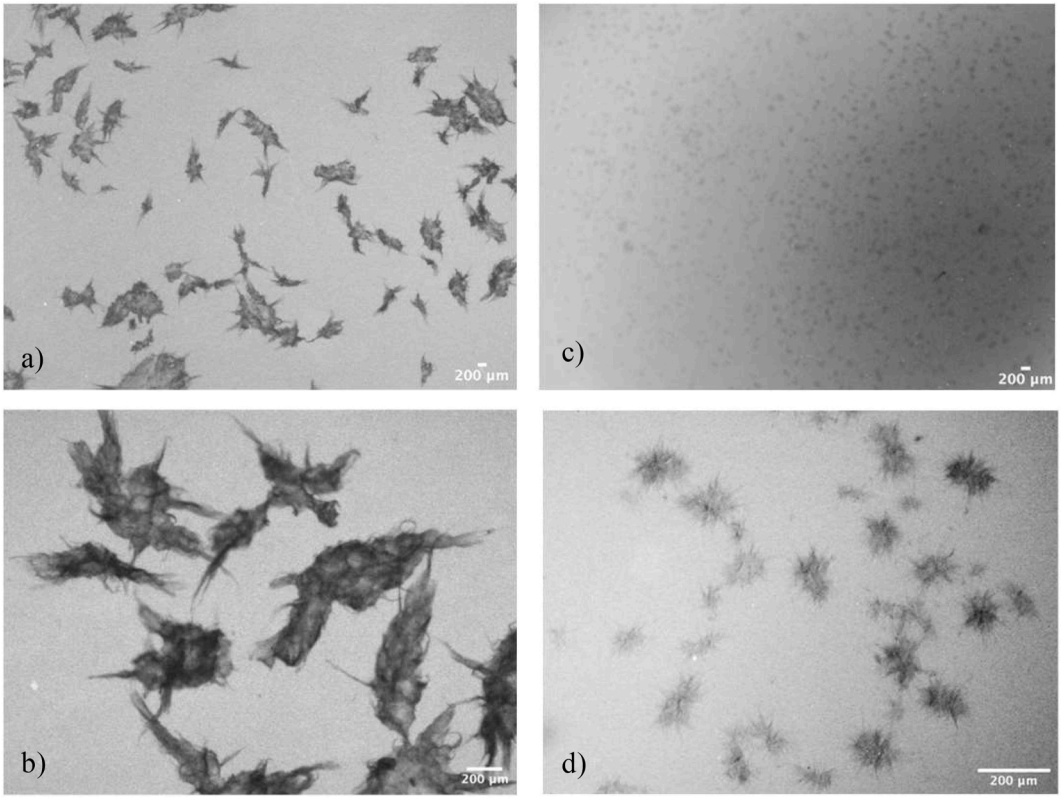

Fig. 2. Micrographs of fluid gel dispersions obtained according to the method described in section 2.1. a) and b) are of LA gellan gum fluid gel particles. c) and d) are of agar fluid gel particles. A different magnification was used between b and d so to better evidence particle microstructural details. The pictures were obtained following the protocol in section 2.7.

We investigated the fluctuation in elastic modulus G′ within the LVR and yield stress σ_y of LA gellan gum fluid gels based on the amplitude sweep method described in section 2.3.1. Our data show that the rheological properties are fluctuating around an average value. A standard deviation of ~15% for the yield stress σ_y (0.6 ± 0.09 Pa) and ~20% for the elastic modulus G' (9.4 ± 1.8 Pa) was observed (Fig. 3a and b), which is remarkably high compared to the typical standard deviation of gels, <1%. Furthermore, after dilution and staining of LA gellan gum fluid gels, performed following the protocol described in section 2.7, we have also observed that when the fluid gel particles sediment, they form a granular pile, angling like a sand pile (Fig. 3c). Furthermore, fluid gels manufactured with no silica show a decrease in G vs number of cycles until reaching an asymptotic behaviour after several cycles were performed (Fig. 3e). Conversely, the instantaneous elastic response G measured from the repeated creep protocol on LA gellan gum fluid gels manufactured with a silica dispersion at a concentration of 7% w/w (Fig. 3f) revealed that G increases progressively with increasing number of cycles.

The presence of conical-shaped structures (Fig. 3c) is a signature of granular materials (Beakawi Al-Hashemi & Baghabra Al-Amoudi, 2018). In addition, the behaviour showed in Fig. 3f is reminiscent of granular materials which pack under gravity when subject to intermittent mechanical solicitations, as reported by Kabla and Debrégeas (2004). The observations showed in Fig. 3e can be attributed to flow-induced abrasion dominated regime in which the fluid gel particles past one another during rejuvenation (section S3, supplementary material), finally causing a decrease in the effective fluid gel particle volume fraction. The magnitude of the observed fluctuations, the formation of granular piles of fluid gel particles and the intermittent packing dynamics suggest that the system can set in different jammed configurations due to its granular matter nature. The system is allowed to reach different available configurations as a result of shear strain above the yield point of the material i.e. through different rejuvenation steps. This is reminiscent of the reversible density fluctuations vs number of taps which have been formerly reported in granular materials (Nowak et al., 1998). These fluctuations (Fig. 3a and b) would not exist in systems that can relax their structure by thermal agitation; they are hence related to the jammed particulated microstructure of fluid gels. Due to the large particle size of granular materials, the thermal activation energy k_bT is negligible compared to the energy required for particle structural rearrangement. Therefore, each metastable packing state will remain persistently unchanged until a sufficiently high external perturbation will alter the particle configuration (Nowak et al., 1998). Indeed, a sufficiently high shear strain applied results in the shear melting of the fluid gel microstructure, whose stress-bearing properties fluctuate (Fig. 3a and b) as a result of different configurations reached at the end of the various rejuvenation steps (Fig. 3d), as observed for granular materials (Howell, Behringer, & Veje, 1999).

3.2. Assessment of physical ageing and ripening in fluid gels

In the present manuscript, the impact of time on fluid gels' rheology and dynamics was investigated probing two hypothesised different contributions: 1) ripening (intra-particle rearrangement and development of the gel network) using the methods specified in sections 2.2 and 2.3.2 for quiescent LA gellan gum gels and LA gellan gum fluid gels, respectively and 2) physical ageing (inter-particle microstructural ordering) using the methods described in section 2.3.3.

3.2.1. Assessment of ripening in fluid gels

We examined the changes on the elastic modulus G' with resting time using the fluid gel ripening protocol described in section 2.3.2 in LA gellan gum fluid gels to investigate the existence of possible ripening effects (Fig. 4), previously observed in quiescently gelled hydrocolloids.

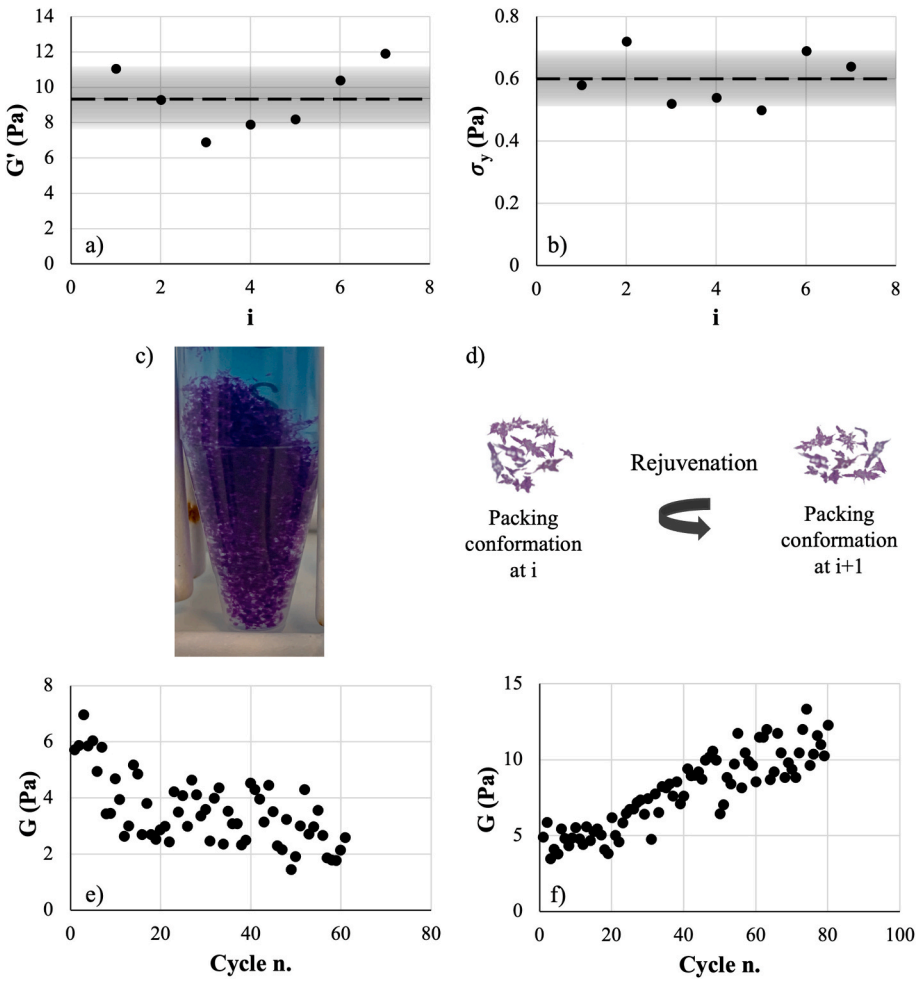

Fig. 3. Values for different repetitions of a) G′ and b) σ_y for the manufactured LA gellan gum fluid gel with repetition number, i, performed on different samples at the same number of cycle (cycle n. = 1). The dashed line indicates the average value, and the gray rectangles represent the standard deviation. c) Picture of LA gellan gum fluid gel particles forming a granular pile after dilution, staining and sedimentation. d) Schematic illustration of the possibility to reach different packing configurations as a result of rejuvenation cycles. Instantaneous elastic response obtained from the repeated creep method as function of number of cycles performed on LA gellan gum fluid gels manufactured with silica dispersions at concentrations of e) 0% w/w and f) 7% w/w.

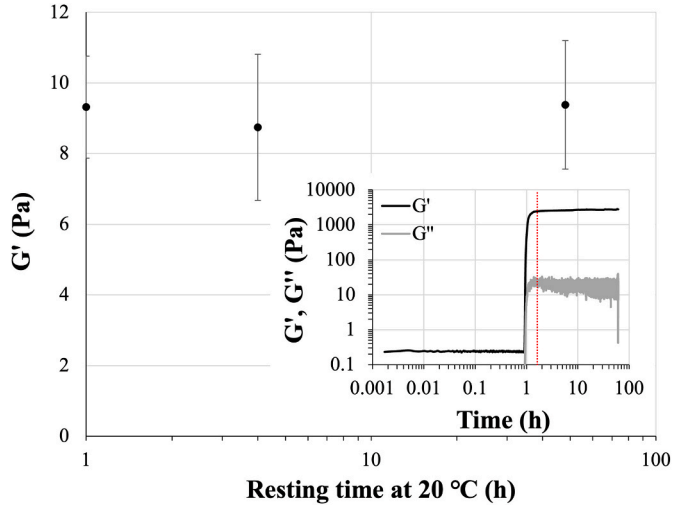

Fig. 4. Evolution of G′ vs resting time for LA gellan gum fluid gels at 20 °C. Before G′ measurement, a rejuvenation step is performed. The error bars indicate the standard deviation of the measurement in triplicate. Inset: evolution of G′ and G" vs time for a quiescently set LA gellan gum gel at 20 °C. The red dotted line indicates the time at which the temperature of 20 °C is reached. (For interpretation of the references to colour in this figure legend, the reader is referred to the Web version of this article.)

In the present study, resting time is defined as the time elapsed from the end of fluid gel production.

At a resting temperature of 20 °C, we did not record any measurable change in G′ over the resting time investigated. Hence, ripening of LA gellan gum fluid gel particles is very small in magnitude and does not contribute to changes in the fluid gel's elastic modulus. This is also supported by the data on ripening of a quiescently set LA gellan gum gel at 20 °C (Fig. 4 inset), which were obtained using the protocol described in section 2.2. G′ increased only ~13% over 59 h. However, an increase in G′(time) has been observed in high methoxyl pectin/sugar (Lopes da Silva & Gonçalves, 1994) and bovine gelatin (Normand et al., 2000) quiescently set gels.

3.2.2. *Assessment of physical ageing in fluid gels*

Our observations from the time sweep protocol described in section 2.3.3 show that the elastic modulus G′ increases linearly with the logarithm of time (Fig. 5). This is consistent with the behaviour of fluid gels as described in the literature (Caggioni et al., 2007; Gabriele et al., 2009; García et al., 2015; Sworn et al., 1995). Gabriele et al. (2009) and Fernández Farrés et al. (2014) initially proposed that the evolution of G'(time) is due to interparticle interactions. In section 3.2.4, we will discuss in more details the mechanism which is likely causing ageing in fluid gels.

We further examined the evolution on fluid gels properties by investigating the relaxation time τ as function of waiting time (t_w) using the repeated creep methodology described in section 2.3.3. As can be observed from Fig. 6, τ probability distributions at different t_w shift to larger values of τ with increasing t_w. In addition, the standard deviations

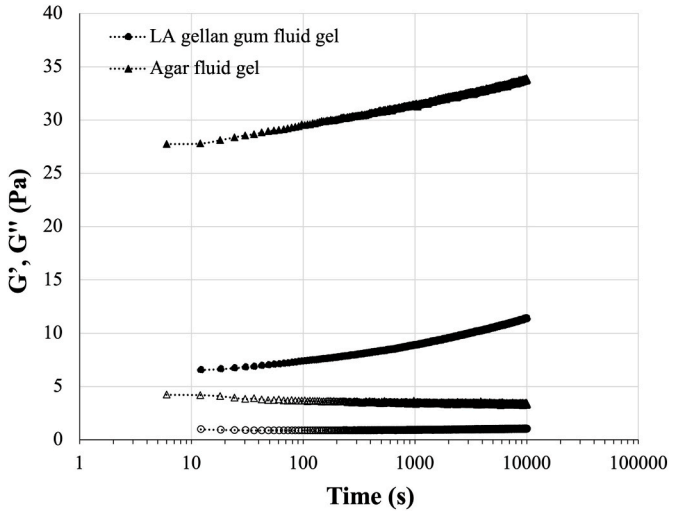

Fig. 5. Evolution of viscoelastic moduli with time of the investigated systems. Full symbols indicate G′ and empty symbols indicate G''.

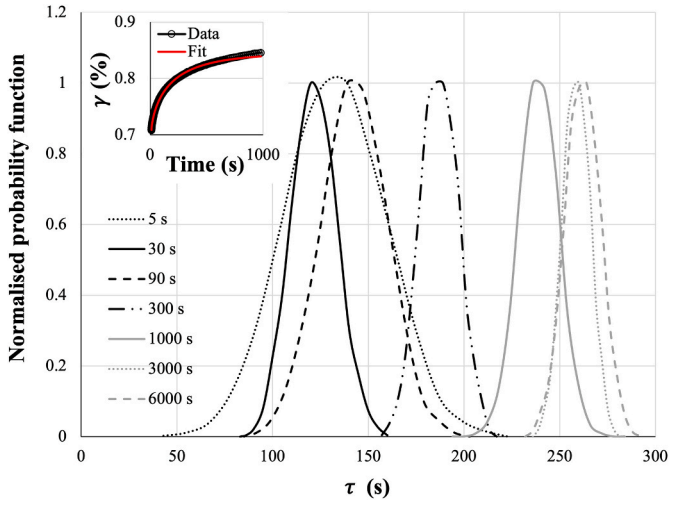

Fig. 6. Normalised probability function fits of $\tau(t_w)$ of the manufactured LA gellan gum fluid gel. The method used to analyse the dataset is explained in section 2.4. The inset shows an example of the creep curve obtained using the repeated creep method and the fit from Equation (1).

of the gaussian distributions progressively reduce with increasing t_w.

The presence of bell-shaped probability data distributions in Fig. 6 implies that: i) the rejuvenation method designed is very effective in erasing the τ evolution caused by physical ageing from cycle to cycle and that ii) fluctuations in fluid gel rheological properties are random.

To better visualise the impact of physical ageing on the dynamics of fluid gels, the average τ was calculated for each t_w dataset obtained using the repeated creep method which is described in section 2.3.3. Thereto, the average τ value was plotted versus the t_w investigated (Fig. 7).

It can be noticed how the average $\tau(t_w)$ increases before converging towards a constant asymptotic value after sufficient t_w has elapsed in LA gellan gum fluid gels. A similar behaviour was observed for $\alpha(t_w)$, where an initial increase was followed by an asymptotic regime. Hence, the relaxation time spectrum becomes narrower and narrower for both systems with increasing t_w, until reaching a stationary width.

Experiments with agar fluid gels, that do not require Ca^{2+} to gel, were carried to test whether ageing only occurred in ion-based fluid gels, or if it was a more general phenomenon in fluid gels. The results showed

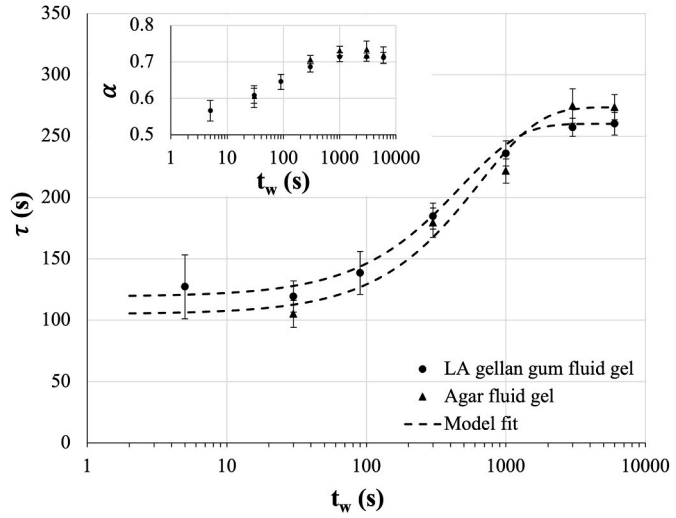

Fig. 7. Relaxation time τ in function of waiting time t_w for the investigated systems. In the inset, the evolution of the stretch exponent α with t_w. The error bars indicate the standard deviation of the measurement based on the number of cycles performed (Table 1).

that agar fluid gels (non-ionic system) behaved very similarly to LA gellan gum fluid gels (ionic system), thus both systems show physical ageing (Fig. 7). This is hence evidence that ageing is not conditioned by phenomena like interparticle divalent ion bridges. The strain amplitude $\gamma_\infty - \gamma_0$ (%), measured from the repeated creep method (section 2.3.3) decreases with longer waiting times t_w both in LA gellan gum and agar fluid gels (Fig. 8).

Although, the agar fluid gels analysed presented a lower creep amplitude compared to the LA gellan gum fluid gels investigated, similarities between the behaviour of the two fluid gels were observed. Comparing Figs. 5 and 8, it can be observed that the value of $\gamma_\infty - \gamma_0$ (t_w) decreases linearly with the logarithm of t_w indicating that the samples are becoming more elastic, as shown in Fig. 5.

3.2.3. *Effect of gravitational field on physical ageing of fluid gels*

Fluid gels of non-colloidal particles sediment and form granular piles (Fig. 3c). As granular matter, their properties might be influenced by gravity, but the extent of the influence has not been explored yet. To test the influence of gravity on fluid gel physical ageing, LA gellan gum fluid

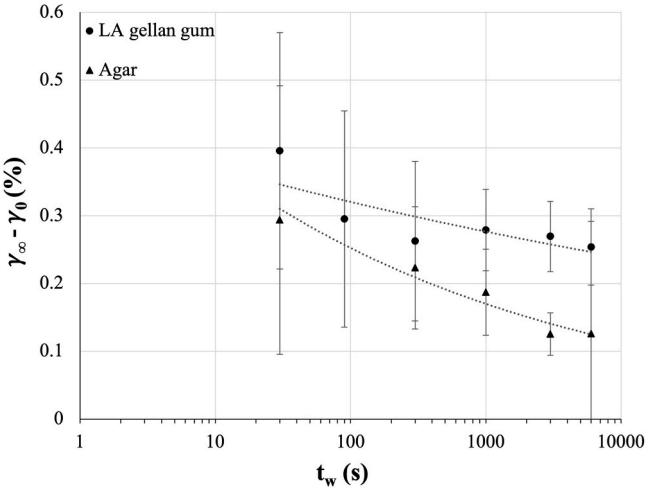

Fig. 8. Strain amplitude (in %) as function of waiting time t_w. The error bars indicate the standard deviation of the measurement based on the number of cycles performed (Table 1).

gels containing silica microparticles were manufactured (section 2.1.2). The LA gellan gum fluid gel particles produced were able to entrap the silica microparticles increasing the fluid gel particle density (Fig. 9). Silica microparticles were chosen as density modifier instead of macromolecules (e.g. polyethylene glycol) because their diffusion over time is very slow and their contribution to the continuous phase viscosity is very low within the very dilute concentration domain (<5%).

Using the repeated creep method (section 2.3.3), we observed that at higher silica concentration (≥ 2% w/w), τ(cycle n.) was not fluctuating around an average value, as expected for fluid gels (Fig. 10a) but, the presence of two regimes was found (Fig. 10b, marked by the red line). In regime 1, the first τ value is higher compared to the $\tau(t_w)$ of reference ($t_w = 90$ s). Then, τ(cycle n.) decreases until reaching regime 2 where, τ(cycle n.) starts to fluctuate around an average value with an increasing level of noise. The shift from regime 1 to regime 2 is due to the transition from a fast-sedimenting fluid gel (regime 1) to progressively compacting fluid gel (regime 2). Indeed, in regime 1, the gravitational stress σ_g (Table 3) is higher than σ_y (~0.6 Pa) causing the fluid gel particles to sediment with time.

The values showed in Table 3 are likely to be underestimated given that fluid gel systems are constituted by soft polydispersed irregularly shaped particles. However, the conclusion that regime 1 is caused by a gravitational stress $\sigma_g >$ fluid gel yield stress σ_y holds until a $\varphi \sim 0.83$ (Table S1, supplementary material). At silica concentrations ≥ 2% w/w, fluid gel particle sedimentation of several tens of millimetres was clearly observed.

The sedimenting fluid gel particles at very short times (the first creep cycle) might have created more interparticle contact points slowing down the creep dynamics. However, from cycle to cycle in regime 1, the sample kept sedimenting and the τ value progressively decreased until $\sigma_g < \sigma_y$. This point represents the onset of region 2 in which the fluid gel compacts under intermittent mechanical solicitations and the τ values starts to fluctuate, as expected. The growing noise of the measurement might be due to the increasing volume packing fraction of the fluid gel particles which makes the system more irreproducible (Fig. 10c and d). At silica concentration of 7 and 10% w/w, higher standard deviations could be caused by an excessively phase separated system, which contributes to add more noise to the measurements.

Thus, using the repeated creep protocol (section 2.3.3) setting the waiting time $t_w = 90$ s, we found that gravity is not playing a role in the fluid gel ageing dynamics within the $\Delta\rho$ range tested, as can be observed from Fig. 11.

These results are not in line with computer simulations of dry granular piles, where gravity was shown to be the way athermal systems relax (Gago & Boettcher, 2020), and with studies of colloidal glasses made of hard nanoparticles spheres in which gravity has been shown to accelerate ageing and retard crystal nucleation (Simeonova & Kegel, 2004). LA gellan gum fluid gels are composed of deformable particles in contrast to colloidal glasses and granular materials formed by hard (undeformable) particles. That large difference in deformability may explain the different behaviours vs gravity effects, between fluid gel particles, and the hard particles used in the granular matter studies of the literature cited. The description of physical ageing in fluid gels is discussed more in detail in section 3.2.4.

3.2.4. *Further considerations and modelling of physical ageing of fluid gels*

The observation of G'(time) increase (Fig. 5) of LA gellan gum fluid gels cannot be attributed to the ripening of the fluid gel particles, neither at short times (1 h after production), nor at longer times (48 h after production), as shown in Fig. 4. In fact, physical ageing has impact on the rheological properties, as shown Figs. 5, 6, 7 and 8. To better understand these changes, the experimental data displayed in Fig. 7 were modelled by a stretched exponential function (Equation (3))

$$\tau(t_w) = (\tau_0 - \tau_\infty)\left[exp\ (-t_w/\tau_s)^\beta\right] + \tau_\infty \quad (3)$$

where τ_0 is the relaxation time after 30 s of waiting time, τ_∞ is the fit relaxation time for an infinite t_w, β is the stretch exponent and was imposed to be equal to 1 and τ_s is the structural relaxation time. τ_s can be seen as the characteristic unit time for structural reorganisation (Joshi & Petekidis, 2018) and was found to be ~ 470 s for LA gellan gum fluid gels and ~ 650 s for agar fluid gels.

The increase in $\tau(t_w)$ reported in Fig. 7 has been formerly observed in various systems like other soft glassy materials (Cipelletti, Manley, Ball, & Weitz, 2000; Cloitre et al., 2000; Negi & Osuji, 2010), molecular glasses (Struik, 1977) and spin glasses (Sibani & Hoffmann, 1989). In addition, we propose that Equation (3) could represent an alternative to the power law model $\tau(t_w) \sim \tau_m^{1-\mu} \cdot t_w^{\mu}$ formerly applied in literature to describe the physical ageing phenomenon occurring in soft glassy materials. The stretch exponent β would then indicate the ageing regime of the investigated system, which in our case it classifies as full ageing, $\beta = 1$ (Joshi & Petekidis, 2018). The exponent α, which relates to the width of the relaxation time distribution for one curve, was found to evolve with time until converging towards an asymptote in both the examined systems. The occurrence of the whole relaxation spectra evolution with t_w were also reported by Baldewa and Joshi (2011), which causes the time-ageing time superposition to not be satisfied (Struik, 1977). The values of α were found to be always lower than 1 indicating a stretched exponential relationship (Fig. 7). In their recent review, Joshi and Petekidis (2018) reported that an exponential ($\alpha = 1$) or a stretched exponential behaviour ($\alpha < 1$) is typically observed when using bulk rheology to probe the system's stress relaxation behaviour. Clearly, in our system, the particles are too large to undergo Brownian motions, and as explained above follow a granular matter behaviour. Because the ageing observed is related to thermally activated motion, it is likely related to the thermal motions of the gel arms of the particles, and more

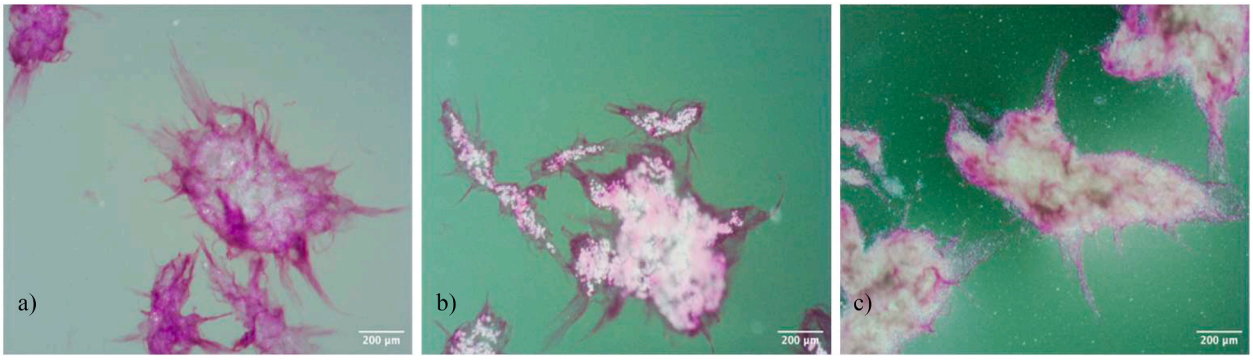

Fig. 9. LA gellan gum fluid gels produced using silica dispersions at a) 0.04%; b) 0.5% and c) 2% w/w. At concentrations ≥ 2% w/w, silica microparticles are also present in the continuous phase. However, most of them are still entrapped in the fluid gel particle. The pictures were acquired following the protocol described in section 2.7. The scale bar is 200 μm on every image.

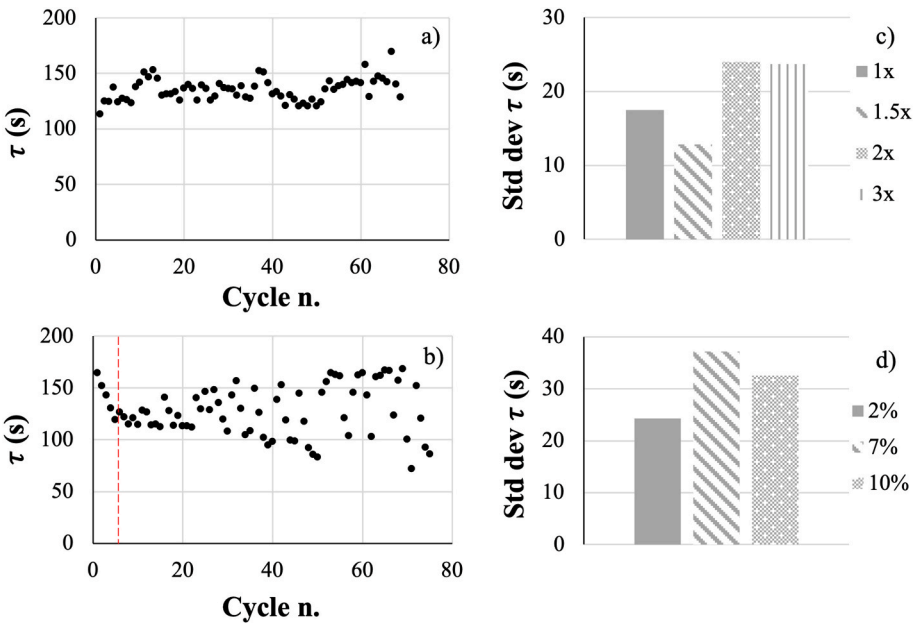

Fig. 10. $\tau(t_w = 90\ s)$ vs number of cycles of a fluid gel produced with a silica dispersion of concentration a) 0.04% and b) 2% w/w. The red dashed line indicates the onset of regime 2 observed for silica concentration ≥ 2% w/w. c) Standard deviation of $\tau(t_w = 90\ s)$ of LA gellan gum fluid gels at different nominal concentrations obtained using the methodology reported in section 2.5 and 2.5.1. d) Standard deviation of $\tau(t_w = 90\ s)$ of LA gellan gum fluid gels manufactured with silica dispersions at different concentrations (% w/w).

Table 3
Calculated gravitational stress σ_g for LA gellan gum fluid gels manufactured with silica microparticle dispersions at different concentrations.

Silica dispersion concentration (% w/w)	0	0.04	0.15	0.5	2	7	10
~ Calculated σ_g (Pa)	0.1	0.2	0.5	1.2	4	17.3	29.1

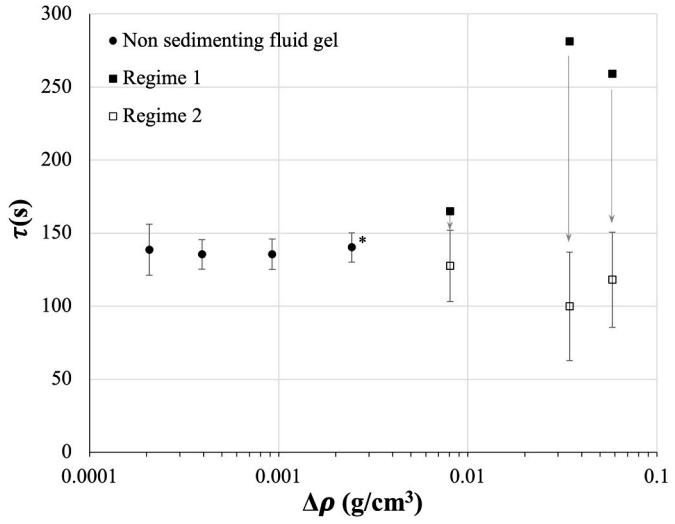

Fig. 11. Impact of gravitational field on $\tau(t_w = 90\ s)$ of LA gellan gum fluid gel. The error bars indicate the standard deviation values of the measurement based on the respective number of cycles performed reported in Table 1 for the lowest $\Delta\rho$ and in Table 2 for the other data points. The asterisk * indicates non fast-sedimenting fluid gels.

precisely, of the time evolution under thermal activation of the contacts between the gel arms. After a macroscopic solicitation, the gel arms are strained, and thus carry some mechanical energy. They will relax progressively this mechanical energy under the effect of thermal activation. This relaxation will slow down – leading to ageing – and will also increase the elastic modulus by increasing the efficiency of the mechanical contacts between gel arms.

Lastly, the asymptotic behaviour in Fig. 7 supports that the ageing driving force(s) progressively fade(s) out in intensity with increasing t_w.

Physical ageing of soft glassy materials is expected to be influenced by all properties of the particles (Joshi, 2014), including their hardness, shape and the interparticle interactions. It should hence not be expected that the results established for quite different systems, e.g. colloidal gels, should hold for the present study, which investigated physical ageing in fluid gels. In addition, more research is needed to elucidate the reasons behind the different behaviour at long ageing times of $\tau(t_w)$, which reaches an asymptotic behaviour (Fig. 7), and G' vs time, which conversely continues to grow (Fig. 5).

4. Conclusion

In this study, we designed a cycle-based method to quantify the intrinsic fluctuation in fluid gels rheological properties, which are due to their granular matter nature. For the first time, we demonstrated the existence of physical ageing in fluid gels made of soft deformable particles, taking the examples of LA gellan gum fluid gels (Ca^{2+}- based fluid gel) and agar fluid gels (non-ionic fluid gel). We observed that the increase in the main relaxation time of the ageing system, $\tau(t_w)$, is neither specific to fluid gels based on ionic bonds (and hence not to related kinetic factors e.g. linked to the diffusion of divalent ions (e.g. Ca^{2+}), nor is induced by gravity effects.

The width of the relaxation time spectrum (the stretch exponent α) showed overall a very similar evolution to τ, with waiting time t_w. In addition, we showed that at long waiting times, τ tends towards a constant asymptotic τ_∞, which suggests that there is a progressive fading out of the driving force intensity. In the present study, we suggest that the driving force for the colloidal ageing could be linked to the presence of the arms, which have colloidal scale, and are the elements of contact between neighbouring fluid gel particles. The structural relaxations themselves may be caused by elastic stresses stored inside the soft deformed particles likely between the arms of the gel particles rather than at the scale of the particles as observed in colloidal systems (Cipelletti & Ramos, 2005; Joshi, 2014; Sudreau et al., 2022), even if this hypothesis deserves further investigation. This study provides a methodology to quantify the effects of physical ageing on fluid gels rheology and dynamics, and more generally a granular matter description of fluid gels. The developed tools, including the modelling of physical ageing, will be very relevant when conducting storage

behaviour studies on applications.

The assessment of the system's natural fluctuations allowed to evidence the absence of significant effects of structural ripening in the fluid gel particles, for the system studied. We suggest that the cycle-based method designed in this study could be applied to investigate physical ageing in other colloidal glasses.

Finally, the results obtained provide knowledge to better tune material properties for specific industrial applications linked to the unique properties of fluid gels.

CRediT authorship contribution statement

Gabriele D'Oria: Conceptualization, Methodology, Validation, Formal analysis, Investigation, Visualization, Writing – Original Draft. Deniz Z. Gunes: Conceptualization, Methodology, Formal analysis, Visualization, Supervision, Funding acquisition, Writing – Review & Editing. François Lequeux: Conceptualization, Methodology, Formal analysis, Visualization, Writing – Review & Editing. Hans Joerg Limbach: Conceptualization, Funding acquisition. Christoph Hartmann: Conceptualization, Funding acquisition. Lilia Ahrné: Conceptualization, Methodology, Formal analysis, Visualization, Supervision, Funding acquisition, Project administration, Writing – Review & Editing.

Declaration of competing interest

The authors declare that they have no known competing financial interests or personal relationships that could have appeared to influence the work reported in this paper.

Data availability

Data will be made available on request.

Acknowledgements

The authors kindly acknowledge Nestlé Research and the Nestlé Institute of Material Sciences for funding this study.

Appendix A. Supplementary data

Supplementary data to this article can be found online at https://doi.org/10.1016/j.foodhyd.2022.108401.

References

Bagheri, L., Mousavi, M. E., & Madadlou, A. (2014). Stability and rheological properties of suspended pulp particles containing orange juice stabilized by gellan gum. *Journal of Dispersion Science and Technology, 35*(9), 1222–1229. https://doi.org/10.1080/01932691.2013.834422

Baldewa, B., & Joshi, Y. M. (2011). Delayed yielding in creep, time–stress superposition and effective time theory for a soft glass. *Soft Matter, 8*(3), 789–796. https://doi.org/10.1039/C1SM06365K

Beakawi Al-Hashemi, H. M., & Baghabra Al-Amoudi, O. S. (2018). A review on the angle of repose of granular materials. *Powder Technology, 330*, 397–417. https://doi.org/10.1016/j.powtec.2018.02.003

Bradbeer, J. F., Hancocks, R., Spyropoulos, F., & Norton, I. T. (2015). Low acyl gellan gum fluid gel formation and their subsequent response with acid to impact on satiety. *Food Hydrocolloids, 43*, 501–509. https://doi.org/10.1016/j.foodhyd.2014.07.006

Brown, C. R. T., Cutler, A. N., & Norton, I. T. (1996). *Liquid based composition comprising gelling polysaccharide capable of forming a reversible gel and a method for preparing such composition (European Union Patent No. EP0355908B1)*. https://patents.google.com/patent/EP0355908B1/en.

Caggioni, M., Spicer, P. T., Blair, D. L., Lindberg, S. E., & Weitz, D. A. (2007). Rheology and microrheology of a microstructured fluid: The gellan gum case. *Journal of Rheology, 51*(5), 851–865. https://doi.org/10.1122/1.2751385

Cassin, G., Appelqvist, I., Normand, V., & Norton, I. T. (2000). Stress-induced compaction of concentrated dispersions of gel particles. *Colloid & Polymer Science, 278*(8), 777–782. https://doi.org/10.1007/s003960000321

Cipelletti, L., Manley, S., Ball, R. C., & Weitz, D. A. (2000). Universal aging features in the restructuring of fractal colloidal gels. *Physical Review Letters, 84*(10), 2275–2278. https://doi.org/10.1103/PhysRevLett.84.2275

Cipelletti, L., & Ramos, L. (2005). Slow dynamics in glassy soft matter. *Journal of Physics: Condensed Matter, 17*(6), R253–R285. https://doi.org/10.1088/0953-8984/17/6/R01

Cloitre, M., Borrega, R., & Leibler, L. (2000). Rheological aging and rejuvenation in microgel pastes. *Physical Review Letters, 85*(22), 4819–4822. https://doi.org/10.1103/PhysRevLett.85.4819

Di Napoli, B., Franco, S., Severini, L., Tumiati, M., Buratti, E., Titubante, M., et al. (2020). Gellan gum microgels as effective agents for a rapid cleaning of paper. *ACS Applied Polymer Materials, 2*(7), 2791–2801. https://doi.org/10.1021/acsapm.0c00342

Ellis, A. L., Mills, T. B., Norton, I. T., & Norton-Welch, A. B. (2019). The effect of sugars on agar fluid gels and the stabilisation of their foams. *Food Hydrocolloids, 87*, 371–381. https://doi.org/10.1016/j.foodhyd.2018.08.027

Emady, H., Caggioni, M., & Spicer, P. (2013). Colloidal microstructure effects on particle sedimentation in yield stress fluids. *Journal of Rheology, 57*(6). https://doi.org/10.1122/1.4824471, 1761–1722.

Ewoldt, R. H., & McKinley, G. H. (2007). Creep ringing in rheometry or how to deal with oft-discarded data in step stress tests. *Rheology Bulletin, 76*(1), 4–6.

Fernández Farrés, I., Douaire, M., & Norton, I. T. (2013). Rheology and tribological properties of Ca-alginate fluid gels produced by diffusion-controlled method. *Food Hydrocolloids, 32*(1), 115–122. https://doi.org/10.1016/j.foodhyd.2012.12.009

Fernández Farrés, I., Moakes, R. J. A., & Norton, I. T. (2014). Designing biopolymer fluid gels: A microstructural approach. *Food Hydrocolloids, 42*, 362–372. https://doi.org/10.1016/j.foodhyd.2014.03.014

Fernández Farrés, I., & Norton, I. T. (2014). Formation kinetics and rheology of alginate fluid gels produced by in-situ calcium release. *Food Hydrocolloids, 40*, 76–84. https://doi.org/10.1016/j.foodhyd.2014.02.005

Fernández Farrés, I., & Norton, I. T. (2015). The influence of co-solutes on tribology of agar fluid gels. *Food Hydrocolloids, 45*, 186–195. https://doi.org/10.1016/j.foodhyd.2014.11.014

Gabriele, A., Spyropoulos, F., & Norton, I. T. (2009). Kinetic study of fluid gel formation and viscoelastic response with kappa-carrageenan. *Food Hydrocolloids, 23*(8), 2054–2061. https://doi.org/10.1016/j.foodhyd.2009.03.018

Gago, P. A., & Boettcher, S. (2020). Universal features of annealing and aging in compaction of granular piles. *Proceedings of the National Academy of Sciences, 117*(52), 33072–33076. https://doi.org/10.1073/pnas.2012757117

García, M. C., Alfaro, M. C., & Muñoz, J. (2015). Yield stress and onset of nonlinear time-dependent rheological behaviour of gellan fluid gels. *Journal of Food Engineering, 159*, 42–47. https://doi.org/10.1016/j.jfoodeng.2015.02.024

García, M. C., Trujillo, L. A., Muñoz, J., & Alfaro, M. C. (2018). Gellan gum fluid gels: Influence of the nature and concentration of gel-promoting ions on rheological properties. ep.fjernadgang.kb.dk *Colloid & Polymer Science, 296*(11), 1741–1748. https://doi.org/10.1007/s00396-018-4396-6.

Garrec, D. A., Guthrie, B., & Norton, I. T. (2013). Kappa carrageenan fluid gel material properties. Part 1: Rheology. *Food Hydrocolloids, 33*(1), 151–159. https://doi.org/10.1016/j.foodhyd.2013.02.014

Garrec, D. A., & Norton, I. T. (2012). Understanding fluid gel formation and properties. *Journal of Food Engineering, 112*(3), 175–182. https://doi.org/10.1016/j.jfoodeng.2012.04.001

Garrec, D. A., & Norton, I. T. (2013). Kappa carrageenan fluid gel material properties. Part 2: Tribology. *Food Hydrocolloids, 33*(1), 160–167. https://doi.org/10.1016/j.foodhyd.2013.01.019

Ghebremedhin, M., Seiffert, S., & Vilgis, T. A. (2021). Physics of agarose fluid gels: Rheological properties and microstructure. *Current Research in Food Science, 4*, 436–448. https://doi.org/10.1016/j.crfs.2021.06.003

Hodge, I. M. (1995). Physical aging in polymer glasses. *Science, 267*(5206), 1945–1947.

Howell, D. W., Behringer, R. P., & Veje, C. T. (1999). Fluctuations in granular media. *Chaos: An Interdisciplinary Journal of Nonlinear Science, 9*(3), 559–572. https://doi.org/10.1063/1.166430

Joshi, Y. M. (2014). Dynamics of colloidal glasses and gels. *Annual Review of Chemical and Biomolecular Engineering, 5*(1), 181–202. https://doi.org/10.1146/annurev-chembioeng-060713-040230

Joshi, Y. M., & Petekidis, G. (2018). Yield stress fluids and ageing. *Rheologica Acta, 57*, 521–549. https://doi.org/10.1007/s00397-018-1096-6

Kabla, A., & Debrégeas, G. (2004). Contact dynamics in a gently vibrated granular pile. *Physical Review Letters, 92*(3), Article 035501. https://doi.org/10.1103/PhysRevLett.92.035501

Lidon, P., Villa, L., & Manneville, S. (2017). Power-law creep and residual stresses in a carbopol microgel. *Rheologica Acta, 56*(3), 307–323. https://doi.org/10.1007/s00397-016-0961-4

Lopes da Silva, J. A., & Gonçalves, M. P. (1994). Rheological study into the ageing process of high methoxyl pectin/sucrose aqueous gels. *Carbohydrate Polymers, 24*(4), 235–245. https://doi.org/10.1016/0144-8617(94)90068-X

Mahdi, M. H., Conway, B. R., Mills, T., & Smith, A. M. (2016). Gellan gum fluid gels for topical administration of diclofenac. *International Journal of Pharmaceutics, 515*(1), 535–542. https://doi.org/10.1016/j.ijpharm.2016.10.048

Negi, A. S., & Osuji, C. O. (2010). Time-resolved viscoelastic properties during structural arrest and aging of a colloidal glass. *Physical Review E, 82*(3), Article 031404. https://doi.org/10.1103/PhysRevE.82.031404

Normand, V., Muller, S., Ravey, J.-C., & Parker, A. (2000). Gelation kinetics of gelatin: A master curve and network modeling. *Macromolecules, 33*(3), 1063–1071. https://doi.org/10.1021/ma9909455

Norton, I. T., Frith, W. J., & Ablett, S. (2006). Fluid gels, mixed fluid gels and satiety. *Food Hydrocolloids, 20*(2), 229–239. https://doi.org/10.1016/j.foodhyd.2004.03.011

Norton, I. T., Jarvis, D. A., & Foster, T. J. (1999). A molecular model for the formation and properties of fluid gels. *International Journal of Biological Macromolecules, 26*(4), 255–261. https://doi.org/10.1016/S0141-8130(99)00091-4

Nowak, E. R., Knight, J. B., Ben-Naim, E., Jaeger, H. M., & Nagel, S. R. (1998). Density fluctuations in vibrated granular materials. *Physical Review E, 57*(2), 1971–1982. https://doi.org/10.1103/PhysRevE.57.1971

Qin, B., Ma, D., Li, F., & Li, Y. (2017). Aqueous clay suspensions stabilized by alginate fluid gels for coal spontaneous combustion prevention and control. *Environmental Science and Pollution Research, 24*(31), 24657–24665. https://doi.org/10.1007/s11356-017-9982-5

Scott, D. W. (2009). Sturges' rule. *WIREs Computational Statistics, 1*(3), 303–306. https://doi.org/10.1002/wics.35

Sibani, P., & Hoffmann, K. H. (1989). Hierarchical models for aging and relaxation of spin glasses. *Physical Review Letters, 63*(26), 2853–2856. https://doi.org/10.1103/PhysRevLett.63.2853

Simeonova, N. B., & Kegel, W. K. (2004). Gravity-induced aging in glasses of colloidal hard spheres. *Physical Review Letters, 93*(3), Article 035701. https://doi.org/10.1103/PhysRevLett.93.035701

Struik, L. C. E. (1977). *Physical aging in amorphous polymers and other materials*.

Sudreau, I., Auxois, M., Servel, M., Lécolier, É., Manneville, S., & Divoux, T. (2022). Residual stresses and shear-induced overaging in boehmite gels. *Physical Review Materials, 6*(4), Article L042601. https://doi.org/10.1103/PhysRevMaterials.6.L042601

Sworn, G., Sanderson, G. R., & Gibson, W. (1995). Gellan gum fluid gels. *Food Hydrocolloids, 9*(4), 265–271. https://doi.org/10.1016/S0268-005X(09)80257-9

Valli, R. C., & Miskiel, F. J. (2001). Gellan gum. In *Handbook of dietary Fibers* (1st ed.). CRC press.

Vanel, L., Howell, D., Winters, D., Behringer, R., & Clément, E. (1999). *Effects of construction history on the stress distribution under a sand pile*. https://doi.org/10.48550/arXiv.cond-mat/9906321. *ArXiv*.

Viasnoff, V., & Lequeux, F. (2002). Rejuvenation and overaging in a colloidal glass under shear. *Physical Review Letters, 89*(6), Article 065701. https://doi.org/10.1103/PhysRevLett.89.065701

Völp, A. R., Kagerbauer, L., Engmann, J., Gunes, D. Z., Gehin-Delval, C., & Willenbacher, N. (2021). In-situ rheological and structural characterization of milk foams in a commercial foaming device. *Journal of Food Engineering, 290*, Article 110150. https://doi.org/10.1016/j.jfoodeng.2020.110150

Willenbacher, N., & Lexis, M. (2018). Foam rheology. In *Foam films and foams*. CRC Press.